

1 Pollutant formation in the pyrolysis and 2 combustion of Automotive Shredder 3 Residue 4

5 *Lorena Rey, Juan A. Conesa*, Ignacio Aracil, Maria A. Garrido, Nuria Ortuño*

6 *Department of Chemical Engineering, University of Alicante, P.O. Box 99, 03080 Alicante, Spain.*

7 *Phone: +(34) 96 590 38 67 Fax: +(34) 96 590 38 26*

8 **Author's email: ja.conesa@ua.es*

9 **ABSTRACT**

10 The present work has been carried out to verify the feasibility of thermal valorization of an
11 automobile shredder residue (ASR). With this aim, the thermal decomposition of this waste has
12 been studied in a laboratory scale reactor, analyzing the pollutants emitted under different
13 operating conditions. The emission factors of carbon oxides, light hydrocarbons, PAHs, PCPhs,
14 PCBzs, PBPhs, PCDD/Fs, dioxin-like PCBs and PBDD/Fs were determined at two temperatures, 600
15 and 850°C, and under different oxygen ratios ranging from 0 (pure pyrolysis) to 1.5 (over-
16 stoichiometric oxidation). After analyzing all these compounds, we conclude that thermal
17 valorization of ASR is a clean way to treat this waste.

18 **Keywords:**

19 ASR; ELV; PCDD/Fs; dl-PCBs; PBDD/Fs; semivolatile compounds

20 1. Introduction

21 In the last decades, the industrial sector devoted to End-of-Life Vehicles (ELV) has changed
22 significantly due to the publication of Directive 2000/53/EC. This evolution has involved a leap from
23 the old scrapyards to the authorized treatment facilities (ATF) (Cossu and Lai, 2015).

24 This Directive established clear objectives of reuse, recovery and recycling of ELV with the aim of
25 reducing the negative effects in the environment. The Directive dictated that “no later than 1st
26 January 2015, for all end-of-life vehicles, the reuse and recovery shall be increased to a minimum of
27 95 % by an average weight per vehicle and year. Within the same time limit, the reuse and recycling
28 shall be increased to a minimum of 85 % by an average weight per vehicle and year” (Cossu and Lai,
29 2015).

30 The EU generates among 7-8 million tons of ELV every year; and it is estimated that the total amount
31 of ELV generated in Europe by 2030 will reach among 14-17 million tons (Andersen et al., 2008;
32 Cossu and Lai, 2015).

33 After depolluting, dismantling and shredding of ELV, a remaining fraction appears. This fraction,
34 called automobile shredder residue (ASR), is a heterogeneous material (Gonzalez-Fernandez et al.,
35 2008; Santini et al., 2011) composed by a complex mixture of plastics (19-35%), rubber (20%), textile
36 (10-40%), wood (2-5%), metals (8%), oils (5%) and other unidentifiable materials (10%) (Morselli et
37 al., 2010). ASR accounts for 10–25% of the initial ELV’s mass and used to be mostly sent to landfill
38 (Gonzalez-Fernandez et al., 2008; Morselli et al., 2010; Reddy et al., 2008; Santini et al., 2011).

39 In order to comply with the European Directive, energy recovery might be feasible using ASR as a
40 secondary fuel in thermal treatments. Some previous work was focused on the energy recovery
41 from the combustible part of ASR. However, there is not extensive information of the emissions
42 from thermal degradation processes of ASR neither in oxidative atmosphere nor inert one. Only

43 some authors (Braslaw et al., 1991; Day et al., 1999; de Marco et al., 2007; Donaj et al., 2009;
44 Galvagno et al., 2001; Zolezzi et al., 2004) characterized the emissions generated in thermal
45 treatments using ASR as raw material so further research is needed to minimize some of the
46 uncertainty regarding the use of such wastes as secondary fuel. Mancini et al. (Mancini et al., 2014a;
47 Mancini et al., 2014b) showed that the slag and bottom ash from the combustion process of ASR
48 can be classified as non-hazardous wastes, according to the EU waste acceptance criteria.
49 Furthermore, the authors recommend to pre-treat the ASR before combustion to increase the heat
50 of combustion by reducing fines, which further enhance dust deposit problems.

51 The aim of the present work is to study the thermal degradation of ASR to assess the emission of
52 pollutants under different operating conditions in a laboratory scale reactor. The study comprises
53 the analysis of CO, CO₂, light hydrocarbons, polycyclic aromatic hydrocarbons (PAHs),
54 polychlorinated phenols (PCPhs), polychlorinated benzenes (PCBzs), polybrominated phenols
55 (PBPhs), polybromo- and polychlorodibenzo- p-dioxins and furans (PBDD/Fs and PCDD/Fs) and
56 dioxin-like polychlorobiphenyls (dl-PCBs). The determination of these compounds is not generally
57 found in the existing literature to the point that some of these contaminants such as PCPhs, PCBzs,
58 PBPhs or PBDD/Fs have not been analyzed for ASR thermal treatments in any previous work. Hence,
59 the present work reports additional findings concerning thermal decomposition of ASR.

60 2. Experimental/Material and Methods

61 2.1. Raw material / ASR

62 The material employed in this study was ASR collected from a cement factory owned by the CEMEX
63 group sited in Alicante (Spain), where it is used as alternative fuel. ASR is a highly heterogeneous
64 material, so prior to its use more than 5 kg of the sample were crushed using immersion in liquid-

65 nitrogen in order to homogenize it, but should be considered for discussion of results that it is very
66 difficult to homogenize.

67 Characterization of this ASR and thermogravimetric study about its thermal decomposition under
68 inert and oxidative atmospheres were previously published (Conesa et al., 2015). The results of the
69 elemental analysis (three repetitions, standard deviation indicated) are: 56.61 ± 2.1 % C, 7.22 ± 0.58
70 % H, 3.73 ± 0.4 % N, 0.01 ± 0.03 % S and 13.36 % O. The ash content is 22.1 wt. % and the moisture
71 of the material is 2.0 wt. %. The net calorific value is 18750 kJ kg^{-1} .

72 Cl^- and Br^- anions were analyzed over five different samples using the EPA Method 5050 by ionic
73 chromatography (DIONEX DX500) and the average values found were 277.0 and 5.56 mg/kg
74 respectively.

75 2.2. Experimental setup

76 A moving tubular reactor was employed to perform the experiments. The reactor consisted of a
77 quartz tube (10 mm internal diameter) where the ASR was uniformly placed in four quartz boats (70
78 mm long each) along the tube. This tube was introduced at an accurately controlled speed in a
79 horizontal furnace while a constant flow of gas was passing through. A detailed description of the
80 system can be found elsewhere (Barneto et al., 2014; Conesa et al., 2011).

81 Combustion and pyrolysis runs were conducted to study ASR decomposition products. During the
82 study, different operating conditions were modified such as temperature, carrier gas and oxygen
83 ratio (Conesa et al., 2009; Conesa et al., 2000).

84 Both pyrolysis and combustion experiments were carried out at two different temperatures, 600
85 and 850°C . The temperature of 850°C was used because it is the temperature reached in the post-
86 combustion treatment plants. Also, the selection of two temperatures was done in order to allow

87 comparing the formation of pollutants in worse conditions to determine the possible ways of their
88 formation / elimination in the combustion process.

89 A sample of approximately 1 g of ASR spread over the four boats was employed in each experiment.
90 For each run, synthetic air (combustion runs) or nitrogen (pyrolysis runs) was introduced in parallel
91 flow to the sample at a constant flow rate of 300 mL min⁻¹ (measured at 20°C, 1 atm).

92 On the other hand, the effect of the presence of oxygen was studied by varying oxygen ratio (λ).
93 This ratio was defined (Aracil et al., 2010) as the fraction between the actual air flow rate and the
94 stoichiometric air flow rate necessary for complete combustion. It is an indicator of the quantity of
95 oxygen present in the process ($\lambda = 0$ for pyrolysis processes, $\lambda = 1$ when the oxygen present is the
96 stoichiometric necessary one for a complete combustion and $\lambda > 1$ for the run with excess of
97 oxygen). The oxygen ratio is easily modified by changing the input speed of the boats. In this sense,
98 the residence time in the hot zone of the furnace is approximately 560 seconds at the minimum
99 input speed (0.5 mm/s) and 150 seconds for the higher input speed (1.9 mm/s), measured at 850
100 °C, as indicated in previous work (Conesa and Domene, 2015).

101 2.3. Sampling and analytical procedure

102 For the pyrolysis and combustion of ASR, the outlet gas stream was sampled to analyze different
103 types of pollutants:

104 - Gases and volatile compounds were collected using Tedlar[®] bags (Restek, USA) for a time long
105 enough to collect all the compounds (Conesa et al., 2009). CO₂, CO, oxygen and nitrogen were
106 analyzed using gas chromatography with thermal conductivity detector (GC-TCD) (Shimadzu GC-
107 14A). Light hydrocarbons (from methane to xylenes) were analyzed by gas chromatography with
108 flame ionization detector (GC-FID) (Shimadzu GC-17A).

109 - Semivolatile organic compounds (PAHs, PCPhs, PCBzs, BrPhs, PCDD/Fs, dl-PCBs and PBDD/Fs) were
110 collected using a polyaromatic Amberlite® XAD-2 resin as adsorbent (Supelco, Bellefonte, USA). It
111 was placed at the exit of the furnace during the entire run. The Tedlar® bags were placed after the
112 XAD-2 resin.

113 The resin was consecutively extracted with toluene, a mixture of dichloromethane/acetone (1:1
114 vol.) and hexane using Accelerated Solvent Extraction (ASE-100, Dionex-Thermo Fisher Scientific
115 Inc., California, USA). The extracted solution was divided into two fractions: 30 wt.% was employed
116 to analyze PAHs (USEPA 8270D method), PCPhs, PCBzs and BrPhs and the other 70 wt.% was used
117 for the analysis of PCDD/Fs, dl-PCBs (EPA 1613 and 1668A methods) and PBDD/Fs (EDF 5408
118 method).

119 The compounds of the first fraction (PAHs, PCPhs, PCBzs and BrPhs) were analyzed by HRGC-MS in
120 a gas chromatograph coupled to a mass spectrometer (Agilent GC 6890N/Agilent MS 5973N, Agilent
121 Technologies, USA).

122 Prior to the analysis of PCDD/Fs, dl-PCBs and PBDD/Fs, a cleanup was performed using an automated
123 clean-up system (Power Prep, FMS, Inc., Boston, MA) with three different columns: silica, alumina,
124 and activated carbon. The purified extract was analyzed by HRGC/HRMS using an Agilent HP5890
125 gas chromatograph equipped with programmable temperature vaporization (PTV) inlet, coupled to
126 a Micromass Autospec Ultima-NT mass spectrometer. For the analysis of PCDD/Fs and dl-PCBs an
127 Agilent DB5-MS chromatographic column (60m×0.25mm×0.25µm) was used, whereas for the
128 analysis of PBDD/Fs a Restek TRB-Meta X5 column (15m×0.25mm×0.25µm) was employed. For
129 PBDD/Fs, the laboratory material was protected from light with aluminum foil throughout the whole
130 experimental process to avoid photodegradation of the brominated compounds.

131 Blank runs in the reactor were performed before each run reproducing the same experimental
132 conditions. This means that a repetition of each run was performed without the ASR sample. Values
133 found in these blank runs were subtracted from the corresponding values of the samples. In a recent
134 paper (Garrido et al., 2016) it was evaluated the reproducibility of similar runs to that presented in
135 this work, where it is shown that the reproducibility is quite good for all kind of compounds analysed
136 in the emissions from pyrolysis and combustion of polyurethane foams.

137 3. Results and discussion

138 3.1. Gases and volatile compounds

139 Results regarding carbon oxides and light hydrocarbons analyzed by GC-TCD and GC-FID for pyrolysis
140 and combustion runs at 600°C and 850°C are shown in Table 1. As stated before, the runs were
141 performed at different values of the oxygen ratio, λ , between 0 and 1.5 approximately.

142 The most remarkable peculiarity in the results shown in Table 1 is the significant amounts of CO and
143 CO₂ in ASR pyrolysis gases; this fact was also reported by other authors (Braslaw et al., 1991; Day et
144 al., 1999; de Marco et al., 2007; Galvagno et al., 2001; Zolezzi et al., 2004). These gases come from
145 the decomposition of polymers such as polycarbonates and polyurethanes present in the ASR and
146 from the decomposition of carbonate fillers present in automotive plastics.

147 With regard to the effect of temperature in pyrolysis experiments, the release of CO increases with
148 temperature meanwhile the CO₂ suffers a slight decrease. This is in agreement with the results
149 presented by Haydary et al. (Haydary et al., 2016), Galvagno et al. (Galvagno et al., 2001) and Zolezzi
150 et al. (Zolezzi et al., 2004) in which they studied the pyrolysis of ASR in different types of reactors.

151 On the other hand, in combustion runs the evolution of CO and CO₂ with temperature for a given λ
152 is not equal for all λ values: for low λ values, CO and CO₂ behave as in pyrolysis runs, indicating that

153 the effect of the temperature is more important than the presence of small amounts of oxygen in
154 the atmosphere; however, at higher λ values the behavior changes, presenting a decrease of CO
155 with temperature while CO₂ increased. This fact indicated that high temperature and high λ values
156 provide a better combustion.

157 It can be also analyzed the evolution of carbon oxides with oxygen ratio at a definite temperature.
158 The expected behavior is that the higher λ , the more CO₂ is present in the gas; and the higher λ , the
159 less CO is present in the gas. This trend is evident in runs at 850°C. Nevertheless, the tendency does
160 not occur at 600°C, where the trend is almost the opposite, although the differences are not as high
161 as in the case of 850°C. Summarizing, the effect of the oxygen ratio is different depending on the
162 temperature considered, similarly to what was observed for the effect of the temperature at a given
163 oxygen ratio.

164 From the data presented, it can be calculated the percentage of the carbon present in the sample
165 that evolves as carbon oxides, i.e., that are converted to CO and CO₂. In the combustion runs, the
166 carbon percentage of the sample evolved as CO is in the range of 0.13 - 13.7%, while the
167 corresponding percentage as CO₂ ranges from 8.9 to 30.9%. In the pyrolysis runs these percentages
168 are logically much lower, ranging from 1.8 - 4.6 for the CO and 4.2 - 5.2 for the CO₂, denoting that
169 major part of the carbon remains in the solid phase (apart from that evolved as hydrocarbons).

170 [Table 1]

171 Regarding the formation of light hydrocarbons, the most abundant compounds are methane,
172 ethylene and propylene for both pyrolysis and combustion runs. Under pyrolytic conditions light
173 hydrocarbons show in general higher yields which indicate that these compounds react with oxygen
174 in combustion experiments (Conesa et al., 2009; Conesa et al., 2000; Fullana et al., 2000). As for the
175 temperature, most of them decrease their yields with increasing temperature, although there are

176 some few exceptions at low (or zero) oxygen ratios, such as the case of methane, ethylene, benzene
177 or toluene. As can be observed in Table 1, the combination of high temperatures and high oxygen
178 ratios implies an important decrease in the volatile compounds yields.

179 3.2. PAHs, PCBzs, PCPhs and PBPhs

180 Figure 1 shows the results on the emissions of PAHs for all the experiments. Data is also available as
181 Supplementary Material in Table SM1. In all the runs the profile of compounds is similar.
182 Naphthalene is clearly the most abundant product, which is in agreement with the results presented
183 by Conesa et al. (Conesa et al., 2009).

184 The maximum formation of the 16 priority PAHs occurs under pyrolytic conditions at high
185 temperature (850°C), as expected since it is known that pyrolytic reactions are the primary source
186 of PAH formation (Thomas and Wornat, 2008). In relation to the effect of temperature, higher yields
187 of PAHs are produced at 850°C in all the experiments, in accordance with previous literature (Fullana
188 et al., 2000), where it is shown that PAHs have maximums at 750-850°C.

189 With respect to the effect of the presence of oxygen, the trend is different depending of the
190 temperature considered. At 850°C, PAHs clearly show a minor emission as the oxygen ratio
191 increases. This indicates that PAHs are pyrolytic products that are easily eliminated in oxygen rich
192 environments at this temperature (Fullana et al., 2000). But at 600°C, the behavior changes. The
193 reason for that can be explained if we consider that, when comparing at the same time both the
194 presence of oxygen and the temperature, two different and competitive behaviors can be observed.
195 At 850°C, an oxidative destruction effect of the PAHs takes place when increasing the oxygen ratio.
196 However, at 600°C the formation of free radicals is enhanced with the presence of oxygen, which
197 boost the pyrolytic reactions. This produces an initial increase in the PAHs yields until stoichiometric

198 conditions followed by a decrease at elevated oxygen ratios when the oxidative destruction effect
199 is dominant (Thomas and Wornat, 2008).

200 [Figure 1]

201 Van Caneghem et al. (Van Caneghem et al., 2010) reported that adding ASR to the refuse-derived
202 fuel (RDF) and wastewater treatment sludge in the usual waste feed to a real-scale fluidized bed
203 combustor not only did not increase the concentration of PAHs in the flue gas but decreased it. Their
204 results showed that the formation of new pollutants during the cooling of the flue gas were
205 independent of the pollutants concentration in the incinerated raw wastes.

206 With regard to PCBzs, PCPhs and PBPhs, relatively low quantities of these compounds were
207 detected. The total emission of chlorobenzenes, chlorophenols and bromophenols are presented in
208 Table 2. The total yields of polychlorinated and polybrominated phenols were nearly negligible and
209 varied between 1-6.6 mg/kg, and 0.2-2.63 mg/kg respectively. Details on each isomer analysis can
210 be found in Supplementary Material (Tables SM2, SM3 and SM4).

211 The emissions from the pyrolysis experiments are lower than those of the combustion experiments
212 at low λ values. That is similar to the behavior observed for PAHs at 600°C. For these λ values, the
213 oxygen favours the formation of free radicals and so pyrolytic reactions that can help to form PCPhs
214 take place. The difference with PAHs is that, since PCPhs are oxygenated compounds, in the case of
215 PCPhs the effect of oxygen in the increase of PCPhs yields is observed also at 850°C, not only at
216 600°C. Finally, the decrease in PCPh yields is only observed at high λ values.”

217 [Table 2]

218 The yields of chlorobenzenes decreased with temperature in combustion experiments meanwhile
219 in pyrolysis the results were in the same order of magnitude at both temperatures, and in general

220 lower than in the presence of oxygen. The most abundant congener was monochlorobenzene as
221 can be found in Table SM3 in the Supplementary Material. Apart from this, no other formation
222 pattern was observed. However, based upon the data presented in Table SM3, it can be stated that
223 an increase in the temperature implies the destruction of such pollutants in the presence of oxygen
224 and so the yields emitted were very low, as expected (Conesa et al., 2009).

225 No many references were found in the literature in order to compare the results obtained for PAHs
226 and no data were found about the formation of chlorobenzenes, chlorophenols and bromophenols
227 in the thermal decomposition of ASR.

228 3.3. PCDD/Fs, dl-PCBs and PBDD/Fs

229 PCDD/Fs and dl-PCBs congener distribution, expressed as pg WHO-TEQ/g, of the different
230 combustion and pyrolysis runs performed are plotted in Figures 2 and 3, respectively. Specific data
231 can be found in Tables SM4 and SM5. Emission factors for PCDD/Fs and PCBs were calculated
232 according to the World Health Organization toxicity equivalence factor (WHO-TEF- 2005) (van den
233 Berg et al., 2006), since it considers the dl-PCBs.

234 [Figures 2 and 3]

235 As can be observed in Fig. 2, in all runs furans contributed more than dioxins to the total emission
236 factor. This is due to the fact that furans have a higher thermal stability than dioxins (Conesa et al.,
237 2002), and of the limited presence of oxygen (Stanmore, 2004).

238 Combustion results show that congener 2,3,4,7,8-PeCDF contributed with the highest value to the
239 total WHO-TEQ. Congener 2,3,4,7,8-PeCDF was found to be the most represented isomer in
240 industrial incinerators emissions (Fiedler et al., 2000). The run with the maximum total emission
241 factor was done at 600°C and $\lambda= 0.9$, with a value of 26077.2 pg WHO-TEQ/g sample burnt.

242 Concerning pyrolysis results, at 600°C congener 2,3,4,7,8-PeCDF contributed with the highest value
243 to the total WHO-TEQ as it occurs in combustion. Whereas, at 850°C, congener 1,2,3,7,8-PeCDD
244 contributed the most to the total WHO-TEQ.

245 As to the emission factor of 2,3,7,8-Cl substituted PCDD/F, in almost every run (at 600°C and 850°C)
246 OCDD and OCDF were the compounds with the highest yields as can be found in Table SM5. This is
247 expected because, at high temperature, the most stable compounds usually are the most
248 chlorinated isomers (Christmann et al., 1989; Kim et al., 2004).

249 Both combustion and pyrolysis experiments at 600 °C generally generated much higher PCDD/F
250 yields (expressed as pg/g) than the runs at 850 °C. This is an expected finding since these compounds
251 are destroyed at high temperatures (Abad et al., 2002; Conesa et al., 2009; Van Caneghem et al.,
252 2010) .

253 In relation to the emissions of the dl-PCBs, as can be found in Table SM6, all combustion and
254 pyrolysis runs at 600°C produced higher yields than at 850°C, being the main congeners PCB-118,
255 PCB-105 and PCB-126. As can be observed in Figure 3 the compounds that contribute the most to
256 the total toxicity are PCB-126 and PCB-169.

257 Several scientific papers have been published reporting PCDD/F emission data from thermal
258 treatments of ASR. Van Caneghem et al. (Van Caneghem et al., 2012) studied the PCDD/F
259 fingerprints of the outputs in a fluidized bed combustor (FBC) in which ASR was co-incinerated with
260 refuse derived fuel (RDF) and wastewater treatment sludge at 850°C. The authors reported the
261 PCDD/F fingerprints of the outputs fractions emitted in the FBC during the ASR co-incineration trial.
262 Total amount of 2,3,7,8-Cl substituted PCDD/F congeners in the gas fraction was approximately
263 30000 pg/g_{DW}, corresponding to approximately 1600 pg I-TEQ/g_{DW}, which is similar to the results
264 shown in the present work. The PCDD/F fingerprints were dominated by PCDFs, mainly HpCDF and

265 OCDF, as it occurs in the present work. Oxygen content has been also confirmed as an important
266 factor influencing the relative abundance of PCDF and PCDD formations: lower oxygen content
267 favors greater amounts of PCDFs than PCDDs (Stanmore, 2004). Moreover Van Caneghem et al.
268 stated that the average copper concentration in the ASR was 5940 mg/kg_{DW}, which is relatively high,
269 might have enhanced PCDD/F formation during the post combustion stage since it is known that
270 copper is a catalyst of the de novo synthesis (Hatanaka et al., 2004; Karstensen, 2008; Lasagni et al.,
271 2009; Ryu et al., 2005). The authors concluded that adding ASR to the RDF and sewage sludge in the
272 usual waste feed to a real-scale fluidized bed combustor increased the concentration of PCDD/Fs in
273 the flue gas.

274 Edo et al. (Edo et al., 2013) studied the performance of the different fractions of the ASR. To do so,
275 combustion trials of the different ASR fractions were conducted at 850°C under substoichiometric
276 oxygen ($\lambda=0.65-0.70$). The authors reported that fines would be the most toxic fraction (800 pg I-
277 TEQ/g), followed by 20–50 mm (298 pg I-TEQ/g) and 50–100 mm (11 pg I-TEQ/g), whereas in the
278 present work, the maximum emission at 850 °C has been 82.9 pg WHO-TEQ/g. Edo et al. also stated
279 the total PCDD/Fs emissions generated by each fraction during the combustion runs: 29000 pg/g
280 dry sample in fines, 14000 pg/g dry sample in 20–50 mm fraction and 4700 pg/g dry sample in 50–
281 100 mm fraction.

282 Joung et al. (Joung et al., 2006) studied the effects of oxygen, catalyst and chlorine content on the
283 formation of PCDD/Fs and dl-PCBs in pyrolysis runs at 600°C. They reported that addition of oxygen
284 to pyrolysis increased by 360 times the I-TEQ of PCDD/Fs, whereas the addition of a catalyst only
285 increased the TEQ by 16 times. In the present work, the addition of limited amount of oxygen also
286 increased very much the emission factor, but the effect is more pronounced at 600 °C, when the
287 conditions are not severe enough to destroy these pollutants. In this way, for PCDD/Fs the effect of

288 oxygen is more pronounced than the effect of catalysts. Regarding dl-PCBs, they found that the total
289 amount of dl-PCBs increased 2.6 times and 12.4 times with either oxygen or a catalyst, respectively.
290 Ishikawa et al. (Ishikawa et al., 2007) studied the PCB emissions during combustion of ASR in a rotary
291 kiln at 850°C. They reported that the I-TEQ for dl-PCB were 110 ng I-TEQ Nm⁻³ (kiln exit) and that
292 the ratios of the TEQ for dl-PCB to the I-TEQ for dioxins at kiln exit were 1.5%.

293 Figure 4 shows the distribution congeners of the PBDD/Fs (“brominated dioxins”), expressed as pg
294 WHO-TEQ/g. In 2013, a joint expert panel from the World Health Organization (WHO) and United
295 Nations Environment Programme (UNEP) proposed the use of similar interim Toxic Equivalence
296 Factors (TEF) for chlorinated and brominated dioxins. Therefore, in this paper total toxic equivalence
297 (TEQ) of PBDD/Fs was calculated according to WHO-TEF- 2005 (van den Berg et al., 2013).

298 [Figure 4]

299 As can be observed in Figure 4, the emission factors of PBDD/Fs at 600°C were higher than at 850°C,
300 as occurred in chlorinated congeners. This fact would show the lower thermal stability of these
301 compounds. The congener that contributed the most to the toxicity of the emissions was the 2,3,7,8-
302 TBDD among dioxins and the 2,3,4,7,8-PeBDF among furans. The run with the highest WHO-TEQ
303 values was that with $\lambda = 0.3$. Nevertheless, the emission factor in pyrolytic conditions is relatively
304 high compared with the PCDD/Fs emissions at 600 °C. Different studies tried to explain the
305 formation and destruction of such pollutants, being for now not clear the formation pathways. For
306 example, Evans and Dellinger (Evans and Dellinger, 2003, 2005) studied the evolution of PBDD/Fs
307 both with temperature and oxygen presence. They also found evidence that some congeners,
308 especially those of furans, decrease in the presence of oxygen, pointing out the significant effect of
309 oxygen on the mechanisms of dioxin and furans formation.

310 Table SM7 in the supplementary material shows the emission factor of 2,3,7,8-Br substituted
311 PBDD/Fs and total WHO₂₀₀₅-TEQ for the emissions of the different combustion and pyrolysis runs
312 performed from the ASR. The most abundant isomer was 1,2,3,4,6,7,8-HpBDF either in combustion
313 and pyrolysis at 600°C as also reported by Ortuño et al. treating electronic wastes (Ortuño et al.,
314 2014).

315 The run with the maximum total emission of PBDD/Fs was that of combustion at 600°C with a $\lambda=$
316 0.3. This is consistent with the study reported by Conesa et al. (Conesa et al., 2009) in which a
317 comparison between the emission rates from pyrolysis and combustion of different wastes was
318 presented, showing that the presence of a small amount of oxygen could promote the formation of
319 some pollutants.

320 No data were found in literature in which brominated dioxin formation in ASR thermal treatments
321 was reported so it was not possible to do a comparison.

322 4. Conclusions

323 In order to better understand the environmental impact during the pyrolysis and combustion of
324 ASR, runs from pure pyrolysis to over-stoichiometric combustion at two different temperatures in a
325 laboratory scale reactor were performed. The products have been analyzed and quantified in order
326 to evaluate whether the thermal valorization of ASR might be feasible. The main conclusions that
327 we can extract from the study are:

- 328 • Significant amounts of CO and CO₂ are generated in pyrolysis. These gases come from the
329 decomposition of polymers (polycarbonates and polyurethanes) present in the ASR and
330 from the decomposition of carbonate fillers present in automotive plastics.

- 331 • The combination of high temperatures and high oxygen ratio causes the drastic reduction
332 of light hydrocarbons.
- 333 • The maximum emissions of the 16 priority PAHs are obtained in pyrolysis at 850 ° C. The
334 most abundant compound, in all experiments, is naphthalene.
- 335 • Chlorobenzenes, chlorophenols and bromophenols yields are almost negligible.
- 336 • The greatest yields of PCDD/Fs, dl-PCBs and PBDD/Fs are obtained at 600°C. Furans
337 contribute more than dioxins to total emissions.
- 338 Based on the results obtained in this study, it can be stated that thermal recovery may be a feasible
339 method for accomplishing the recovery rates established in the Directive 2000/53/EC.

340 Acknowledgments

341 Support for this work was provided by the CTQ2013-41006-R project from the Ministry of Economy
342 and Competitiveness (Spain) and the PROMETEOII/2014/007 project from the Valencian Community
343 Government (Spain). The authors are grateful to CEMEX ESPAÑA, S.A. for supplying the samples.

344 References

345

- 346 Abad, E., Adrados, M.A., Caixach, J., Rivera, J., 2002. Dioxin abatement strategies and mass balance
347 at a municipal waste management plant. *Environ. Sci. Technol.* 36, 92-99.
- 348 Andersen, F., Larsen, H., Skovgaard, M., 2008. Projection of end-of-life vehicles: development of a
349 projection model and estimates for ELVs for 2005-2030, Copenhagen.
- 350 Aracil, I., Font, R., Conesa, J.A., 2010. Chlorinated and nonchlorinated compounds from the pyrolysis
351 and combustion of polychloroprene. *Environ. Sci. Technol.* 44, 4169-4175.
- 352 Barneto, A.G., Moltó, J., Ariza, J., Conesa, J.A., 2014. Thermogravimetric monitoring of oil refinery
353 sludge. *Journal of Analytical and Applied Pyrolysis* 105, 8-13.
- 354 Braslaw, J., Melotik, D.J., Gealer, R.L., Wingfield Jr, R.C., 1991. Hydrocarbon generation during the
355 inert gas pyrolysis of automobile shredder waste. *Thermochimica Acta* 186, 1-18.

356 Conesa, J.A., Domene, A., 2015. Gasification and pyrolysis of *Posidonia oceanica* in the presence of
357 dolomite. *Journal of Analytical and Applied Pyrolysis* 113, 680-689.

358 Conesa, J.A., Font, R., Fullana, A., Martín-Gullón, I., Aracil, I., Gálvez, A., Moltó, J., Gómez-Rico, M.F.,
359 2009. Comparison between emissions from the pyrolysis and combustion of different wastes.
360 *Journal of Analytical and Applied Pyrolysis* 84, 95-102.

361 Conesa, J.A., Fullana, A., Font, R., 2000. Tire pyrolysis: Evolution of volatile and semivolatile
362 compounds. *Energy Fuels* 14, 409-418.

363 Conesa, J.A., Fullana, A., Font, R., 2002. De novo synthesis of PCDD/F by thermogravimetry. *Environ.*
364 *Sci. Technol.* 36, 263-269.

365 Conesa, J.A., Galvez, A., Martín-Gullón, I., Font, R., 2011. Formation and Elimination of Pollutant
366 during Sludge Decomposition in the Presence of Cement Raw Material and Other Catalysts.
367 *Advances in Chemical Engineering Science* 1, 183-190.

368 Conesa, J.A., Rey, L., Aracil, I., 2015. Modeling the thermal decomposition of automotive shredder
369 residue. *J. Therm. Anal. Calorim.* 124, 317-327.

370 Cossu, R., Lai, T., 2015. Automotive shredder residue (ASR) management: An overview. *Waste*
371 *Manage. (Oxford)* 45, 143-151.

372 Christmann, W., Kasiske, D., Kloppel, K.D., Partscht, H., Rotard, W., 1989. Combustion of
373 polyvinylchloride - An important source for the formation of PCDD/PCDF. *Chemosphere* 19, 387-
374 392.

375 Day, M., Shen, Z., Cooney, J.D., 1999. Pyrolysis of auto shredder residue: experiments with a
376 laboratory screw kiln reactor. *Journal of Analytical and Applied Pyrolysis* 51, 181-200.

377 de Marco, I., Caballero, B.M., Cabrero, M.A., Laresgoiti, M.F., Torres, A., Chomón, M.J., 2007.
378 Recycling of automobile shredder residues by means of pyrolysis. *Journal of Analytical and Applied*
379 *Pyrolysis* 79, 403-408.

380 Donaj, P., Yang, W., Blasiak, W., Forsgren, C., 2009. Kinetic study of decomposition of ASR residues
381 after pyrolysis in inert and oxidative atmosphere, Joint Conference: International Thermal
382 Treatment Technologies (IT3) and Hazardous Waste Combustors (HWC), pp. 465-483.

383 Edo, M., Aracil, I., Font, R., Anzano, M., Fullana, A., Collina, E., 2013. Viability study of automobile
384 shredder residue as fuel. *J. Hazard. Mater.* 260, 819-824.

385 Evans, C.S., Dellinger, B., 2003. Mechanisms of Dioxin Formation from the High-Temperature
386 Pyrolysis of 2-Bromophenol. *Environmental Science & Technology* 37, 5574-5580.

387 Evans, C.S., Dellinger, B., 2005. Mechanisms of Dioxin Formation from the High-Temperature
388 Oxidation of 2-Bromophenol. *Environmental Science & Technology* 39, 2128-2134.

389 Fiedler, H., Lau, C., Eduljee, G., 2000. Statistical analysis of patterns of PCDDs and PCDFs in stack
390 emission samples and identification of a marker congener. *Waste Management and Research* 18,
391 283-292.

392 Fullana, A., Font, R., Conesa, J.A., Blasco, P., 2000. Evolution of products in the combustion of scrap
393 tires in a horizontal, laboratory scale reactor. *Environ. Sci. Technol.* 34, 2092-2099.

394 Galvagno, S., Fortuna, F., Cornacchia, G., Casu, S., Coppola, T., Sharma, V.K., 2001. Pyrolysis process
395 for treatment of automobile shredder residue: Preliminary experimental results. *Energy Convers.*
396 *Manage.* 42, 573-586.

397 Garrido, M.A., Font, R., Conesa, J.A., 2016. Pollutant emissions during the pyrolysis and combustion
398 of flexible polyurethane foam. *Waste Manage. (Oxford)* 52, 138-146.

399 Gonzalez-Fernandez, O., Hidalgo, M., Margui, E., Carvalho, M.L., Queralt, I., 2008. Heavy metals'
400 content of automotive shredder residues (ASR): Evaluation of environmental risk. *Environ. Pollut.*
401 153, 476-482.

402 Hatanaka, T., Kitajima, A., Takeuchi, M., 2004. Role of copper chloride in the formation of
403 polychlorinated dibenzo-p-dioxins and dibenzofurans during incineration. *Chemosphere* 57, 73-79.

404 Haydary, J., Susa, D., Gelingher, V., Čacho, F., 2016. Pyrolysis of automobile shredder residue in a
405 laboratory scale screw type reactor. *Journal of Environmental Chemical Engineering* 4, 965-972.

406 Ishikawa, Y., Noma, Y., Yamamoto, T., Mori, Y., Sakai, S.i., 2007. PCB decomposition and formation
407 in thermal treatment plant equipment. *Chemosphere* 67, 1383-1393.

408 Joung, H.T., Seo, Y.C., Kim, K.H., 2006. Effects of oxygen, catalyst and PVC on the formation of PCDDs,
409 PCDFs and dioxin-like PCBs in pyrolysis products of automobile residues. *Chemosphere* 65, 1481-
410 1489.

411 Karstensen, K.H., 2008. Formation, release and control of dioxins in cement kilns. *Chemosphere* 70,
412 543-560.

413 Kim, K.S., Hong, K.H., Ko, Y.H., Kim, M.G., 2004. Emission Characteristics of PCDD/Fs, PCBs,
414 Chlorobenzenes, Chlorophenols, and PAHs from Polyvinylchloride Combustion at Various
415 Temperatures. *Journal of the Air and Waste Management Association* 54, 555-562.

416 Lasagni, M., Collina, E., Grandesso, E., Piccinelli, E., Pitea, D., 2009. Kinetics of carbon degradation
417 and PCDD/PCDF formation on MSWI fly ash. *Chemosphere* 74, 377-383.

418 Mancini, G., Viotti, P., Luciano, A., Fino, D., 2014a. On the ASR and ASR thermal residues
419 characterization of full scale treatment plant. *Waste Manage. (Oxford)* 34, 448-457.

420 Mancini, G., Viotti, P., Luciano, A., Raboni, M., Fino, D., 2014b. Full scale treatment of ASR wastes in
421 a modified rotary kiln. *Waste Manage. (Oxford)* 34, 2347-2354.

422 Morselli, L., Santini, A., Passarini, F., Vassura, I., 2010. Automotive shredder residue (ASR)
423 characterization for a valuable management. *Waste Manage. (Oxford)* 30, 2228-2234.

424 Ortuño, N., Conesa, J.A., Molto, J., Font, R., 2014. Pollutant emissions during pyrolysis and
425 combustion of waste printed circuit boards, before and after metal removal. *Sci. Total Environ.* 499,
426 27-35.

427 Reddy, M.S., Kurose, K., Okuda, T., Nishijima, W., Okada, M., 2008. Selective recovery of PVC-free
428 polymers from ASR polymers by ozonation and froth flotation. *Resources, Conservation and*
429 *Recycling* 52, 941-946.

430 Ryu, J.-Y., Mulholland, J.A., Takeuchi, M., Kim, D.-H., Hatanaka, T., 2005. CuCl₂-catalyzed PCDD/F
431 formation and congener patterns from phenols. *Chemosphere* 61, 1312-1326.

432 Santini, A., Morselli, L., Passarini, F., Vassura, I., Di Carlo, S., Bonino, F., 2011. End-of-Life Vehides
433 management: Italian material and energy recovery efficiency. *Waste Manage. (Oxford)* 31, 489-494.

434 Stanmore, B.R., 2004. The formation of dioxins in combustion systems. *Combust. Flame* 136, 398-
435 427.

436 Thomas, S., Wornat, M.J., 2008. The effects of oxygen on the yields of polycyclic aromatic
437 hydrocarbons formed during the pyrolysis and fuel-rich oxidation of catechol. *Fuel* 87, 768-781.

438 Van Caneghem, J., Block, C., Vermeulen, I., Van Brecht, A., Van Royen, P., Jaspers, M., Wauters, G.,
439 Vandecasteele, C., 2010. Mass balance for POPs in a real scale fluidized bed combustor co-
440 incinerating automotive shredder residue. *J. Hazard. Mater.* 181, 827-835.

441 Van Caneghem, J., Vermeulen, I., Block, C., Van Brecht, A., Van Royen, P., Jaspers, M., Wauters, G.,
442 Vandecasteele, C., 2012. Destruction and formation of PCDD/Fs in a fluidised bed combustor co-
443 incinerating automotive shredder residue with refuse derived fuel and wastewater treatment
444 sludge. *J. Hazard. Mater.* 207-208, 152-158.

445 van den Berg, M., Birnbaum, L.S., Denison, M., De Vito, M., Farland, W., Feeley, M., Fiedler, H.,
446 Hakansson, H., Hanberg, A., Haws, L., Rose, M., Safe, S., Schrenk, D., Tohyama, C., Tritscher, A.,
447 Tuomisto, J., Tysklind, M., Walker, N., Peterson, R.E., 2006. The 2005 World Health Organization
448 reevaluation of human and mammalian toxic equivalency factors for dioxins and dioxin-like
449 compounds. *Toxicol. Sci.* 93, 223-241.

450 van den Berg, M., Denison, M.S., Birnbaum, L.S., DeVito, M., Fiedler, H., Falandysz, J., Rose, M.,
451 Schrenk, D., Safe, S., Tohyama, C., Tritscher, A., Tysklind, M., Peterson, R.E., 2013. Polybrominated

452 Dibenzo-p-dioxins (PBDDs), Dibenzofurans (PBDFs) and Biphenyls (PBBs) - Inclusion in the Toxicity
453 Equivalency Factor Concept for Dioxin-like Compounds. *Toxicol. Sci.*
454 Zolezzi, M., Nicoletta, C., Ferrara, S., Iacobucci, C., Rovatti, M., 2004. Conventional and fast pyrolysis
455 of automobile shredder residues (ASR). *Waste Manage. (Oxford)* 24, 691-699.

456

457

458

FIGURE CAPTIONS AND TABLE LEGENDS

Table 1. Emissions of gases and volatile compounds.

Table 2. Total emissions of chlorobenzenes, chlorophenols and bromophenols

Figure 1. Emissions of PAHs (mg/kg sample).

Figure 2. Distribution congeners of the PCDD/Fs (pg WHO-TEQ/g)

Figure 3. Dioxin-like PCBs emission factor (pg WHO-TEQ/g)

Figure 4. Distribution congeners of the PBDD/Fs (pg WHO-TEQ/g)

Table 1. Emissions of gases and volatile compounds.

	Experiment									
	600°C					850°C				
	Pyrolysis	Combustion				Pyrolysis	Combustion			
	$\lambda=0$	$\lambda=0.35$	$\lambda=0.56$	$\lambda=0.96$	$\lambda=1.56$	$\lambda=0$	$\lambda=0.32$	$\lambda=0.55$	$\lambda=0.98$	$\lambda=1.54$
<i>Compound</i>	mg compound/kg sample burnt (ppm)									
<i>Analysis by GC-TCD</i>										
CO ₂	108700	515500	419800	352700	186200	86900	470300	505800	641700	382000
CO	37300	119600	125000	140200	69500	94600	284500	211800	64300	2700
R _{CO} = CO/(CO + CO ₂)	0.255	0.188	0.229	0.284	0.272	0.521	0.377	0.295	0.091	0.007
<i>Analysis by GC-FID</i>	mg compound/kg sample burnt (ppm)									
methane	20200	8780	9340	6760	1450	69800	42200	155	2830	
ethane	10900	1790	1730	920	142	5230	2260	6770	89.7	
ethylene	24200	18600	26600		6550	96800	60300		3420	
propane	5520	788	671	230	30.5	341	107			
propylene	75200	35100	33000	16200	2830	29800	8520	327	282	
n-butane	531	257		142	24.0			42.9	74.4	
trans-2-butene	5120									
cis-2-butene	6830	188		90.3	135	121	223			
1.3-butadiene					128				48.3	
2-butino	64.3									
n-hexane	1310	76.5					1110			
benzene	47.3	6590	6480	4610	1620	18500	2360	3080	2300	16.2
toluene	15700					39000	18600			
xilene (p-m-o-)		3420			460					

Table 2. Total emissions of chlorobenzenes, chlorophenols and bromophenols

	Experiment									
	600°C					850°C				
	Pyrolysis	Combustion				Pyrolysis	Combustion			
	$\lambda=0$	$\lambda=0.35$	$\lambda=0.56$	$\lambda=0.96$	$\lambda=1.56$	$\lambda=0$	$\lambda=0.32$	$\lambda=0.55$	$\lambda=0.98$	$\lambda=1.54$
	mg compound/kg sample burnt (ppm)									
Total PCPh	1	4.8	6.6	0.03	0.2	2.2	5.7	3.9	0.1	0.4
Total PCBz	4.94	213	237	303	245	18	63	14	14	1.72
Total PBPh	1.15	0.2	1.04	1.13	2.63	0.04	0.07	0.06	0.03	0.11

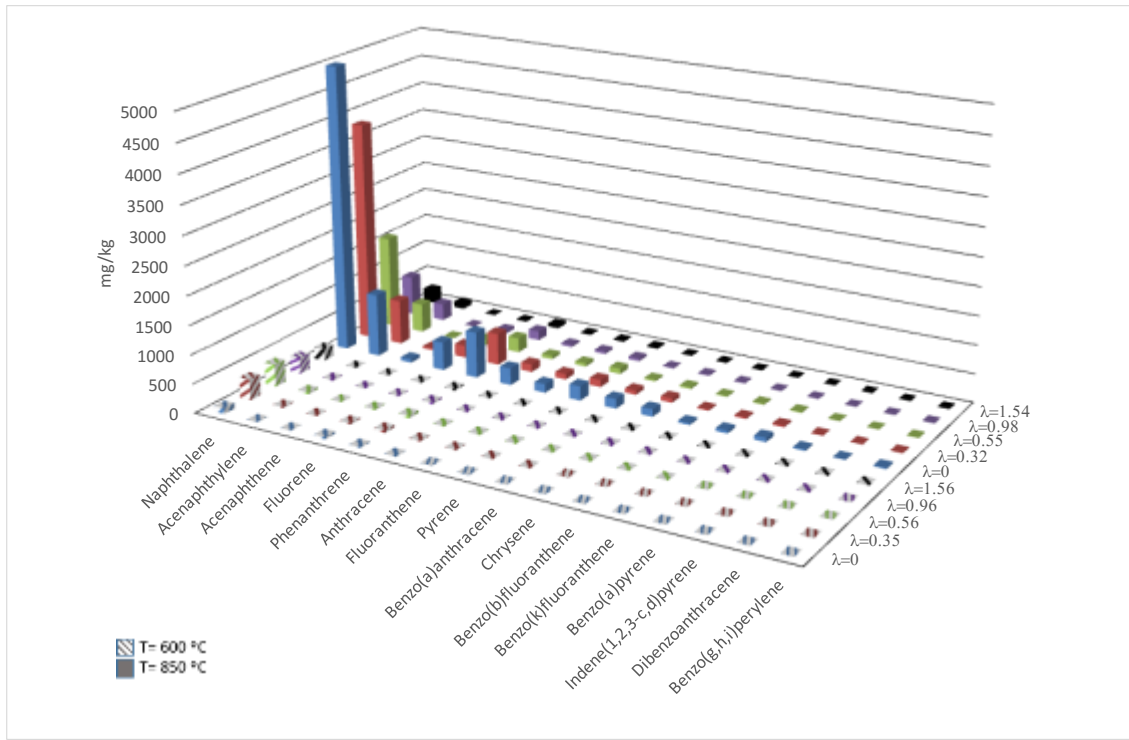


Figure 1. Emissions of PAHs (mg/kg sample).

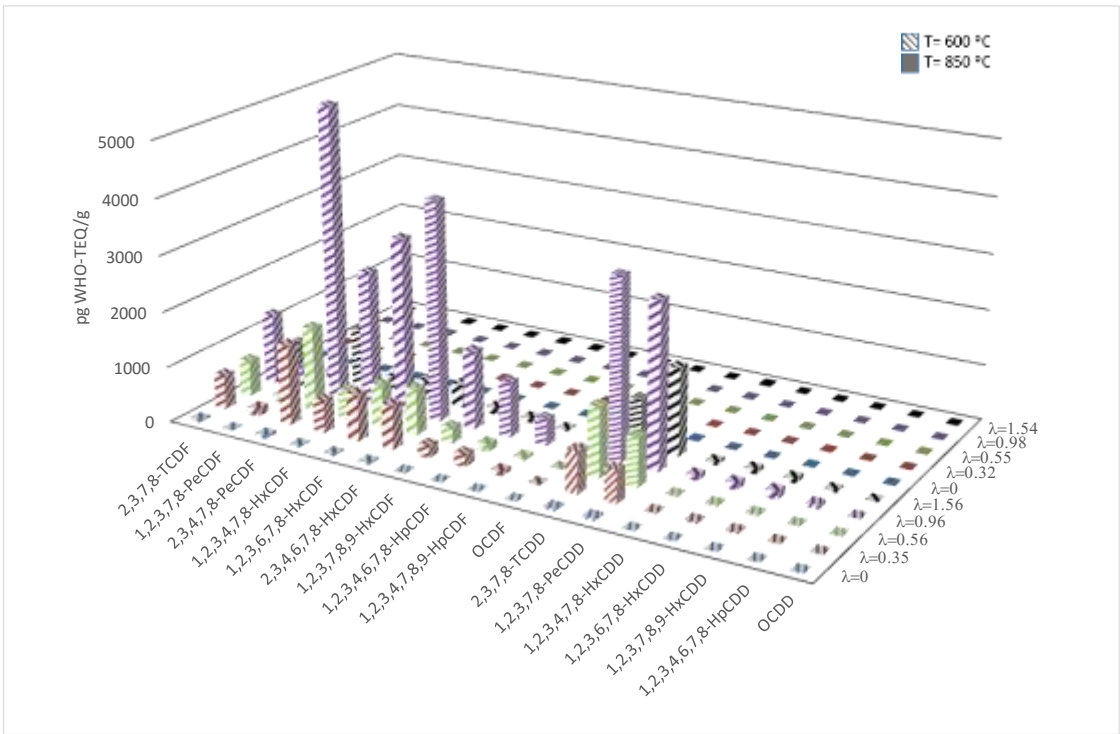


Figure 2. Distribution congeners of the PCDD/Fs (pg WHO-TEQ/g)

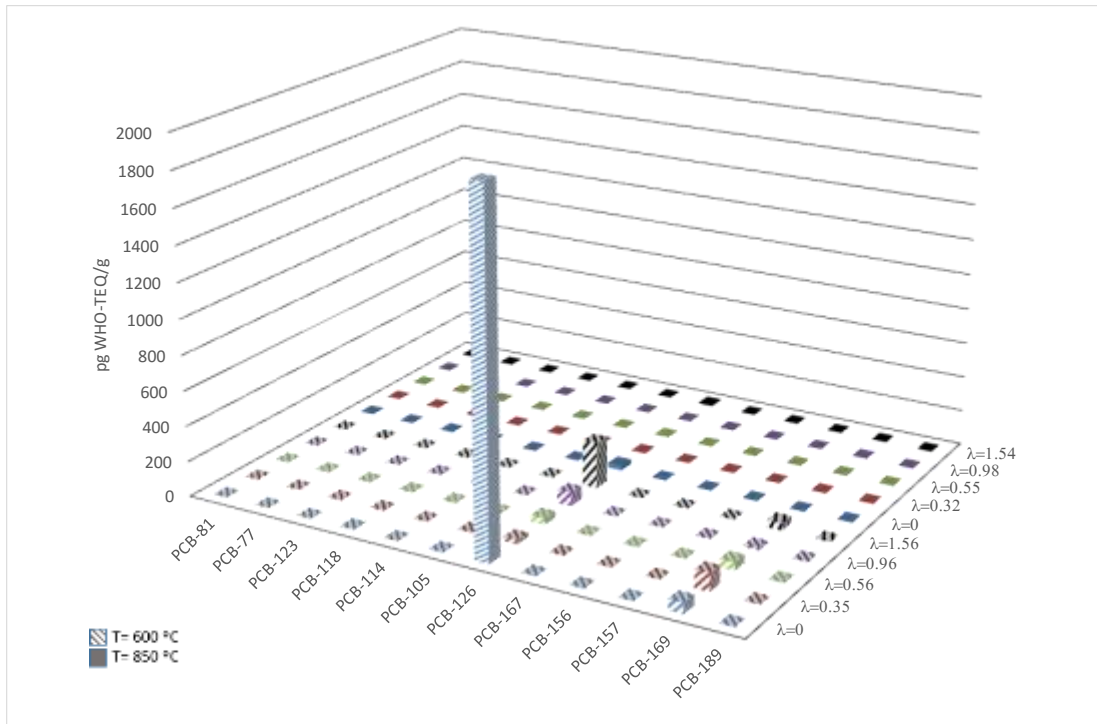


Figure 3. Dioxin-like PCBs emission factor (pg WHO-TEQ/g)

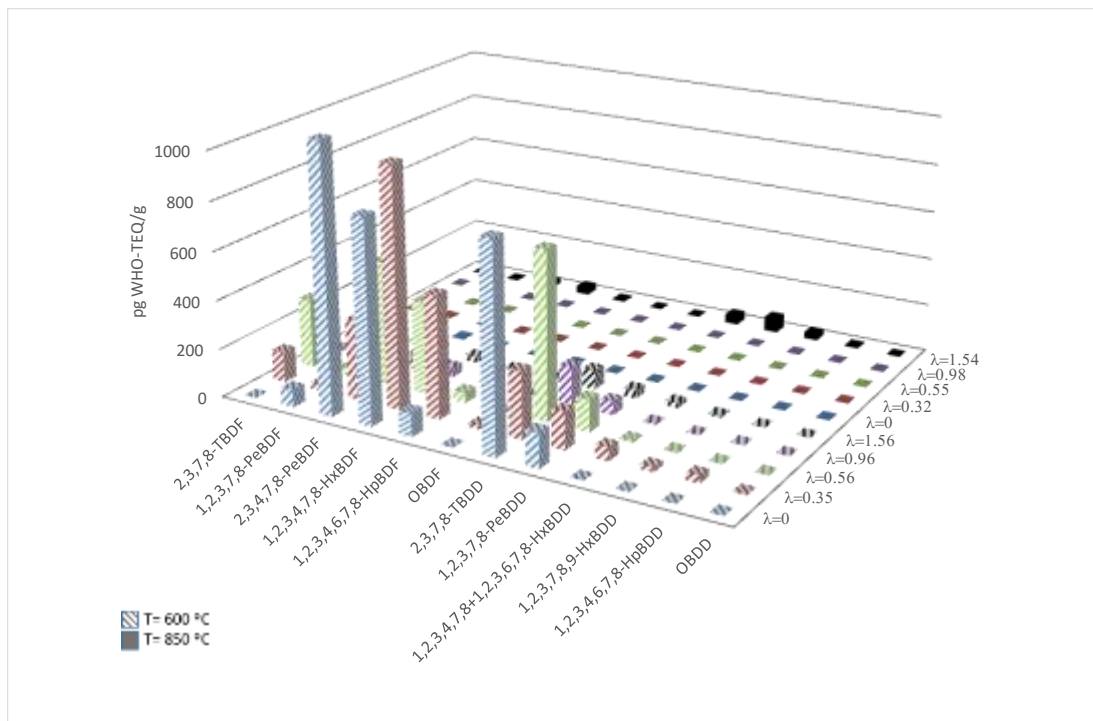


Figure 4. Distribution congeners of the PBDD/Fs (pg WHO-TEQ/g)

Supplementary material

Table SM1. Yields of US EPA priority PAHs in the pyrolysis and combustion of ASR.

	Experiment									
	600°C					850°C				
	Pyrolysis	Combustion				Pyrolysis	Combustion			
	$\lambda=0$	$\lambda=0.35$	$\lambda=0.56$	$\lambda=0.96$	$\lambda=1.56$	$\lambda=0$	$\lambda=0.32$	$\lambda=0.55$	$\lambda=0.98$	$\lambda=1.54$
mg compound/kg sample burnt (ppm)										
Naphthalene	96.1	358	385	271	202	5540	3840	1610	689	239
Acenaphthylene	4.0	16.0	34.3	18.0	5.0	1100	779	504	295	106
Acenaphthene	4.0	6.0	5.0	3.0	2.0	63.0	40.0	11.0	4.0	1.0
Fluorene	35.4	20.1	17.1	9.0	8.0	493	213	99.0	54.0	13.0
Phenanthrene	15.7	41.5	45.4	30.6	27.8	799	556	253	160	63.0
Anthracene	9.0	12.4	10.9	6.0	3.5	295	137	59.4	37.8	12.9
Fluoranthene	4.6	7.6	10.0	6.6	4.6	151	96.2	58.3	43.4	18.7
Pyrene	5.3	4.2	5.6	9.4	2.5	250	126	92.7	47.4	23.9
Benzo(a)anthracene	3.6	3.1	3.2	5.1	1.0	166	72.3	27.1	11.4	3.8
Chrysene	4.2	5.4	7.4	8.7	3.0	130	75.7	30.7	13.5	5.8
Benzo(b)fluoranthene	2.4	1.4	2.3	4.4	1.1	36.3	21.7	13.1	6.8	2.1
Benzo(k)fluoranthene	1.1	0.70	1.2	2.1	0.45	52.6	24.0	16.5	6.2	0.90
Benzo(a)pyrene	1.3	0.60	1.0	1.8	0.33	75.5	25.8	15.9	4.8	1.8
Indene(1,2,3-c,d)pyrene	-	-	-	-	-	27.0	7.0	5.0	2.0	1.0
Dibenzoanthracene	-	-	-	-	-	9.0	3.1	2.3	-	-
Benzo(g,h,i)perylene	-	-	-	-	-	19.0	6.0	6.0	4.0	2.0

Table SM2. Yields of bromophenols in the pyrolysis and combustion of ASR.

	Experiment									
	600°C					850°C				
	Pyrolysis	Combustion				Pyrolysis	Combustion			
	$\lambda=0$	$\lambda=0.35$	$\lambda=0.56$	$\lambda=0.96$	$\lambda=1.56$	$\lambda=0$	$\lambda=0.32$	$\lambda=0.55$	$\lambda=0.98$	$\lambda=1.54$
mg compound/kg sample burnt (ppm)										
2-	0.20	0.05	0.99	1.1	2.6	0.01	0.06	0.03	0.01	0.04
3-+4-	-	-	-	-	-	-	-	0.03	0.02	0.07
2,4-	0.09	0.01	0.01	0.01	0.03	-	-	-	-	-
2,3-+2,5-	0.04	0.01	0.01	-	-	-	-	-	-	-
2,6-	0.75	0.04	0.01	0.02	0.02	0.02	0.01	-	-	-
3,5-	-	-	-	-	-	-	-	-	-	-
3,4-	-	-	-	-	-	-	-	-	-	-
2,3,5-	0.01	-	0.01	-	-	-	-	-	-	-
2,4,6-	0.03	-	-	-	-	0.01	-	-	-	-
2,3,4-	-	-	0.01	-	-	-	-	-	-	-
2,4,5-	0.01	0.01	-	-	-	-	-	-	-	-
2,3,6-	-	-	-	-	-	-	-	-	-	-
3,4,5-	-	-	-	-	-	-	-	-	-	-
2,3,5,6-	0.01	0.04	-	-	-	-	-	-	-	-
2,3,4,5-+2,3,4,6-	0.01	0.04	-	-	-	-	-	-	-	-
penta-	-	-	-	-	-	-	-	-	-	-
Total mono-BrPh	0.20	0.05	0.99	1.1	2.6	0.01	0.06	0.06	0.03	0.11
Total di-BrPh	0.88	0.06	0.03	0.03	0.05	0.02	0.01	-	-	-
Total tri-BrPh	0.05	0.01	0.02	-	-	0.01	-	-	-	-
Total tetra-BrPh	0.02	0.08	-	-	-	-	-	-	-	-
Total penta-BrPh	-	-	-	-	-	-	-	-	-	-
TOTALS	1.2	0.20	1.0	1.1	2.6	0.04	0.07	0.06	0.03	0.11

Table SM3. Yields of chlorobenzenes in the pyrolysis and combustion of ASR.

	Experiment									
	600°C					850°C				
	Pyrolysis	Combustion				Pyrolysis	Combustion			
	$\lambda=0$	$\lambda=0.35$	$\lambda=0.56$	$\lambda=0.96$	$\lambda=1.56$	$\lambda=0$	$\lambda=0.32$	$\lambda=0.55$	$\lambda=0.98$	$\lambda=1.54$
mg compound/kg sample burnt (ppm)										
mono-	4.6	204	231	289	199	17.3	62.8	13.4	13.3	1.5
1,3-	0.02	0.96	0.98	1.7	5.4	0.10	0.12	0.05	0.02	-
1,4-	0.08	3.2	1.9	2.1	4.6	0.12	0.14	0.07	0.03	0.01
1,2-	0.08	2.3	1.8	3.9	13.2	0.12	0.13	0.13	0.01	0.04
1,3,5-	-	0.07	0.06	0.19	0.61	-	0.01	-	0.01	-
1,2,4-	0.10	1.8	0.78	2.5	7.7	0.06	0.02	0.27	0.53	0.12
1,2,3-	-	0.23	0.16	2.1	8.8	0.19	0.01	0.01	-	0.01
1,2,3,5-+1,2,4,5-	0.01	0.20	0.08	0.55	1.8	0.03	0.01	-	-	-
1,2,3,4-	0.08	0.15	0.07	0.56	2.2	0.08	0.01	-	-	0.01
penta-	-	0.07	0.05	0.29	0.96	0.01	0.01	-	0.01	0.02
hexa-	0.01	-	-	0.04	0.19	-	-	0.01	0.01	0.02
Total mono-ClBz	4.6	204	231	289	199	17.3	62.8	13.4	13.3	1.5
Total di-ClBz	0.18	6.5	4.7	7.7	23.2	0.34	0.39	0.25	0.06	0.05
Total tri-ClBz	0.10	2.1	1.0	4.8	17.1	0.25	0.04	0.28	0.54	0.13
Total tetra-ClBz	0.09	0.35	0.15	1.1	4.0	0.11	0.02	-	-	0.01
Total penta-ClBz	-	0.07	0.05	0.29	0.96	0.01	0.01	-	0.01	0.02
Total hexa-ClBz	0.01	-	-	0.04	0.19	-	-	0.01	0.01	0.02
TOTALS	5.0	213	237	303	245	18.0	63.3	13.9	13.9	1.7

Table SM4. Yields of chlorophenols in the pyrolysis and combustion of ASR.

	Experiment									
	600°C					850°C				
	Pyrolysis	Combustion				Pyrolysis	Combustion			
	$\lambda=0$	$\lambda=0.35$	$\lambda=0.56$	$\lambda=0.96$	$\lambda=1.56$	$\lambda=0$	$\lambda=0.32$	$\lambda=0.55$	$\lambda=0.98$	$\lambda=1.54$
mg compound/kg sample burnt (ppm)										
2-	-	-	-	-	-	-	-	-	-	-
3-+4-	-	-	-	-	-	-	-	-	-	-
2,4-	-	-	-	2.4	17.0	-	-	0.03	0.05	0.03
2,5-	-	-	-	-	6.8	-	-	0.03	-	-
2,3-	1.0	1.2	1.4	0.27	0.70	0.14	-	-	-	-
2,6-	-	-	-	1.6	4.6	-	-	-	0.01	-
3,5-	-	3.6	5.0	-	-	2.1	5.7	3.9	-	0.32
3,4-	-	-	-	-	-	-	-	-	-	-
2,3,5-	-	-	-	0.04	5.2	-	-	-	-	-
2,4,6-	-	-	0.19	0.42	6.2	-	-	-	-	-
2,4,5-	-	-	-	0.05	0.24	-	-	-	-	-
2,3,4-	-	-	-	-	0.22	-	-	-	-	-
2,3,6-	-	-	-	-	-	-	-	-	-	-
3,4,5-	-	-	-	-	-	-	-	-	-	-
2,3,5,6-	-	-	-	0.02	0.22	-	-	-	0.01	-
2,3,4,5-	-	-	-	-	-	-	-	-	-	-
2,3,4,6-	-	-	-	0.10	0.72	-	-	0.01	0.04	0.02
penta-	-	-	-	0.03	0.17	-	-	-	0.05	0.03
Total mono-ClPh	-	-	-	-	-	-	-	-	-	-
Total di-ClPh	1.0	4.8	6.4	4.3	29.1	2.2	5.7	4.0	0.06	0.35
Total tri-ClPh	-	-	0.19	0.51	11.9	-	-	-	-	-
Total tetra-ClPh	-	-	-	0.12	0.94	-	-	0.01	0.05	0.02
Total penta-ClPh	-	-	-	0.03	0.17	-	-	-	0.05	0.03
TOTALS	1.0	4.8	6.6	5.0	42.1	2.2	5.7	4.0	0.16	0.40

Table SM5. Yields of PCDD/Fs in the pyrolysis and combustion of ASR.

	Experiment									
	600°C					850°C				
	Pyrolysis	Combustion				Pyrolysis	Combustion			
	$\lambda=0$	$\lambda=0.35$	$\lambda=0.56$	$\lambda=0.96$	$\lambda=1.56$	$\lambda=0$	$\lambda=0.32$	$\lambda=0.55$	$\lambda=0.98$	$\lambda=1.54$
pg compound/g sample burnt (ppt)										
2,3,7,8-TCDF	412	6200	6480	12800	5010	61.6	270	-	-	-
1,2,3,7,8-PeCDF	272	4830	4350	12600	2310	11.1	88.9	-	-	3.1
2,3,4,7,8-PeCDF	196	4820	5070	17700	3400	17.7	29.0	20.9	24.6	30.5
1,2,3,4,7,8-HxCDF	208	5750	5060	24400	2640	-	56.2	31.1	26.9	63.7
1,2,3,6,7,8-HxCDF	248	8320	7550	31700	3300	-	37.7	22.5	41.8	73.6
2,3,4,6,7,8-HxCDF	305	7850	8280	39500	4100	-	23.9	55.2	115	171
1,2,3,7,8,9-HxCDF	120	2180	2820	14100	1250	-	-	55.4	97.6	127
1,2,3,4,6,7,8-HpCDF	484	22200	13200	98300	7480	44.1	-	176	342	581
1,2,3,4,7,8,9-HpCDF	136	7720	4720	47000	2220	25.3	-	-	97.7	148
OCDF	182	23800	9390	192300	7360	-	483	681	1070	1150
2,3,7,8-TCDD	37.7	749	1250	3260	866	1.5	18.7	-	-	-
1,2,3,7,8-PeCDD	45.3	578	874	2970	1570	9.3	-	-	8.4	17.5
1,2,3,4,7,8-HxCDD	-	109	162	877	500	-	-	-	-	10.3
1,2,3,6,7,8-HxCDD	-	232	227	1160	767	-	-	-	-	13.9
1,2,3,7,8,9-HxCDD	-	211	231	1400	749	-	-	-	-	12.3
1,2,3,4,6,7,8-HpCDD	148	789	653	6810	3010	9.7	-	27.4	-	94.8
OCDD	347	1250	-	12700	2690	-	-	111	268	323

Table SM6. Yields of PCBs in the pyrolysis and combustion of ASR.

	Experiment									
	600°C					850°C				
	Pyrolysis	Combustion				Pyrolysis	Combustion			
	$\lambda=0$	$\lambda=0.35$	$\lambda=0.56$	$\lambda=0.96$	$\lambda=1.56$	$\lambda=0$	$\lambda=0.32$	$\lambda=0.55$	$\lambda=0.98$	$\lambda=1.54$
pg compound/g sample burnt (ppt)										
PCB-81	1790	1460	843	1360	3240	479	12.6	4.5	2.1	24.7
PCB-77	10400	9130	6950	7760	12500	4960	-	-	12.5	118
PCB-123	9420	11100	4790	4920	5400	2020	37.4	5.0	-	1.9
PCB-118	92700	77900	49100	41500	40000	13900	282	67.7	-	32.7
PCB-114	1910	1330	828	840	1270	289	1.7	-	-	7.4
PCB-105	43400	31500	21100	18700	17000	4670	50.7	-	-	12.8
PCB-126	19900	216	348	735	2570	249	15.9	11.6	-	56.4
PCB-167	5420	4730	2650	2090	2270	407	-	-	-	5.8
PCB-156	9670	10600	5490	4620	4810	629	-	-	9.8	28.5
PCB-157	3300	3310	2520	1370	1610	163	-	-	5.9	15.1
PCB-169	1980	3350	1500	346	1390	-	-	3.5	23.3	14.4
PCB-189	223	169	509	244	476	19.2	-	5.6	12.1	24.6

Table SM7. Yields of PBDD/Fs in the pyrolysis and combustion of ASR.

	Experiment									
	600°C					850°C				
	Pyrolysis	Combustion				Pyrolysis	Combustion			
	$\lambda=0$	$\lambda=0.35$	$\lambda=0.56$	$\lambda=0.96$	$\lambda=1.56$	$\lambda=0$	$\lambda=0.32$	$\lambda=0.55$	$\lambda=0.98$	$\lambda=1.54$
pg compound/g sample burnt (ppt)										
2,3,7,8-TBDF	-	1260	2860	98.1	87.7	-	-	-	-	10.1
1,2,3,7,8-PeBDF	1640	820	907	57.5	1120	-	-	-	2.6	80.4
2,3,4,7,8-PeBDF	2480	1100	1710	153	65.1	16.0	-	-	3.8	84.4
1,2,3,4,7,8-HxBDF	7470	9870	3800	410	237	-	-	4.4	11.1	321
1,2,3,4,6,7,8-HpBDF	9600	50300	4170	1100	369	-	14.4	10.7	31.5	576
OBDF	-	47300	422	639	193	-	-	-	-	382
2,3,7,8-TBDD	755	274	693	157	77.2	-	-	-	-	2.7
1,2,3,7,8-PeBDD	143	152	133	54.1	34.3	-	-	-	-	37.2
1,2,3,4,7,8+1,2,3,6,7,8-HxBDD	-	530	69.9	43.6	189	-	-	-	-	598
1,2,3,7,8,9-HxBDD	-	181	35.4	28.1	64.0	-	-	-	-	267
1,2,3,4,6,7,8-HpBDD	-	2900	92.1	126	113	-	18.8	13.5	14.9	527
OBDD	-	5530	-	-	94.8	-	-	-	-	774